

Research Article

**Enhancement of String Tension Using Thin-Film Metallic Glass Coatings**Yi-Chia Liao <sup>1, ‡</sup>, Chun-Hway Hsueh <sup>1</sup>, Wen-Shin Lee <sup>2, \*</sup>

1. Department of Materials Science and Engineering, National Taiwan University, No. 1, Sec. 4, Roosevelt Rd., Taipei 10617, Taiwan; E-Mails: yichia.liao09@gmail.com; hsuehc@ntu.edu.tw
2. Department of Athletics, National Taiwan University, No. 1, Sec. 4, Roosevelt Rd., Taipei 10617, Taiwan; E-Mail: apple@ntu.edu.tw

‡ Current Affiliation: Integrated Service Technology Inc., Hsinchu City 30078, Taiwan

\* **Correspondence:** Wen-Shin Lee; E-Mail: apple@ntu.edu.tw**Academic Editor:** Waseem Haider**Special Issue:** [Recent Advances in Metallic Glass](#)*Recent Progress in Materials*  
2020, volume 2, issue 2  
doi:10.21926/rpm.2002014**Received:** May 16, 2020  
**Accepted:** June 8, 2020  
**Published:** June 15, 2020**Abstract**

Inspired by the application of metallic glass sheet as face material for improving the performance of golf clubs, the present work was aimed to explore the application of thin-film metallic glass (TFMG) coatings for enhancing the performance of strings. In order to achieve this aim, badminton strings were coated with TFMG coatings of different thicknesses. The compositions of these TFMG coatings were analyzed using an electron probe micro-analyzer. The amorphous structure of the film was verified using X-ray diffraction. In order to simulate the strung tension of the string in the racquet, the coated string was subjected to different pounds of tensile loading and was subsequently impacted by a steel ball to study both energy loss and the coefficient of restitution (COR). It was observed that while the TFMG coatings could reduce the energy loss and increase the COR at impact, they exerted negligible effects on the tensile strength of the string. In addition, there existed an optimum coating thickness, beyond which cracking of the coating would occur, degrading the beneficial effects of the coating.



© 2020 by the author. This is an open access article distributed under the conditions of the [Creative Commons by Attribution License](#), which permits unrestricted use, distribution, and reproduction in any medium or format, provided the original work is correctly cited.

## Keywords

Metallic glass; coating; tension; elastic properties; coefficient of restitution

## 1. Introduction

Badminton is one of the popular sports. It can be played as a leisure activity or for a professional competition, and is reported to have the fastest ball speed among the racquet sports [1]. This high ball speed is attributed to the network weaving and tension of the badminton strings. Previously, badminton strings were prepared from the sheep guts. With developments in the manufacturing technology for the strings, natural guts were replaced by artificial braid fibers, which had low prices, good functional playability, and adequate durability. The constituents of the braided strings are nylon, polyester, and synthetic [2]. A novel type of badminton string with titanium thin-film coating was manufactured by YONEX Co. Ltd. [3]. This string exhibits high tension and provides the players with a feeling of sharpness and comfort, along with a short control time and strong offensiveness. These strings are suitable for tournament players with an emphasis on control.

Metallic glass, a novel amorphous alloy with excellent mechanical properties such as high hardness, high elastic strain limit, good wear and corrosion resistance, high strength, and good fatigue properties, was first reported by Klement et al. in 1960 [4]. Since then, it has been explored and developed rigorously [5-9]. Owing to its excellent mechanical properties, metallic glass has found application in sports equipment, such as the golf club, tennis rackets, baseball bats, skis, snowboards, and scuba gear [9-11]. For instance, Zr-based metallic glass with a thickness of approximately 4-5 mm, used as the face material in the golf clubs, exhibits high energy transfer of 99% from the club head to the ball, much higher than those exhibited by stainless steel (60%) and Ti alloy (70%). The maximum flying distance of the golf ball was 225 m when hit using a metallic glass face, while it was only 213 m when hit using the Ti-alloy face [5, 6]. Metallic glasses, in the form of thin films, i.e., thin film metallic glasses (TFMGs), have also been developed [12-14]. In recent times, TFMGs have been applied to micro-electro-mechanical system devices, medical tools, diffusion barriers, and biosensors, etc. [15-25].

The main objective of the present study was to explore the application of TFMG coatings to improve the performance of badminton strings. In order to achieve this objective, badminton strings were coated with either Zr-based or Ti-based TFMG coatings of different thicknesses using sputtering. The compositions of the TFMG coatings were analyzed using an electron probe micro-analyzer (EPMA). The amorphous structure of the coatings was verified using X-ray diffraction, while the morphologies of the TFMG coatings were observed under a microscope. In order to simulate the strung tension of the string in the racquet, the coated string was subjected to different pounds of tensile loading (in the range of 18-26 lb) and was subsequently impacted by a steel ball to study both energy loss and the coefficient of restitution (COR) at impact. A video camera was employed to record the positions of the steel ball during the impact and the rebound processes. The effects of the TFMG coatings on the tensile strength of the badminton string were also examined.

## 2. Materials and Methods

### 2.1 Thin-Film Metallic Glasses and Sputtering

A direct current (DC) magnetron sputter was used for film deposition. In order to achieve uniform coating thickness on a flat substrate, the substrate holder was rotated with respect to the revolution axis, as illustrated schematically in Figure 1. However, in order to deposit a uniform coating on the rounded surface of the string, a home-made string holder was attached to the substrate holder to rotate the string with respect to the rotation axis (Figure 1); this was in addition to the rotation of the substrate holder with respect to the revolution axis. In order to prepare the TFMG coatings with different thicknesses, Zr-based and Ti-based TFMGs were coated on the BG65 (YONEX Co. Ltd) strings through the process of sputtering at the power of 100 W for 5 min, 30 min, 60 min, and 120 min. The base pressure of the chamber was maintained below  $5 \times 10^{-7}$  torr, while the working pressure was  $5 \times 10^{-3}$  torr. Strings with a diameter of 0.7 mm and a length of 15 cm were cleaned sequentially with alcohol and de-ionized water in an ultrasonic cleaner for at least twenty minutes each, followed by being fixed on the designed fixture. The coated portion of each string was 5 cm in length. Silicon (Si) wafers were also placed on the substrate holder together with the string holder, and the films deposited on the Si wafers were used to analyze compositions and structures.

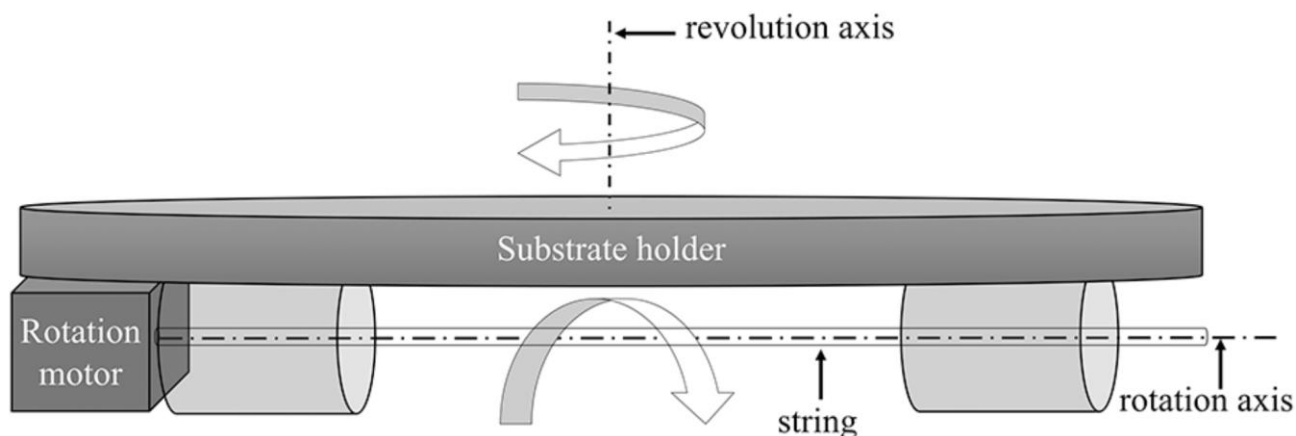


**Figure 1** Schematic drawing illustrating the rotation of the substrate holder with respect to the revolution axis and depicting the home-made string holder for rotating the string with respect to the rotation axis.

### 2.2 Characterizations

The compositions of the as-deposited films on the Si wafers were examined using an electron probe micro-analyzer (EPMA, JXA-8200F, JEOL, Japan). The structures were verified using X-ray diffraction (XRD, Rigaku TTRAX 3) with the incidence grazing angle of  $2^\circ$ . The thickness of the film was examined using a scanning electron microscope (SEM, NOVA 450, FEI, USA), while the morphologies of the TFMGs coated on the strings were observed under an optical microscope (OM, AXIO A1, ZEISS, Germany).

### 2.3 Modified Ball-Drop Test and Strength Measurements

The ball-drop test [26-28] was originally developed to characterize the restitution of a collision between the ball and the target, i.e., how much of the kinetic energy remains for the ball to rebound from the target versus how much of the energy is lost as heat or as the work done to deform the objects. In the normal ball-drop test, the ball is dropped vertically to impact a flat target, and the rebound height of the ball is recorded using a video camera [26, 27]. However, in the present study, the impact between a ball and a single string was to be considered, which would not render it feasible to adopt the normal ball-drop test. Therefore, the test was modified to suit our purpose.

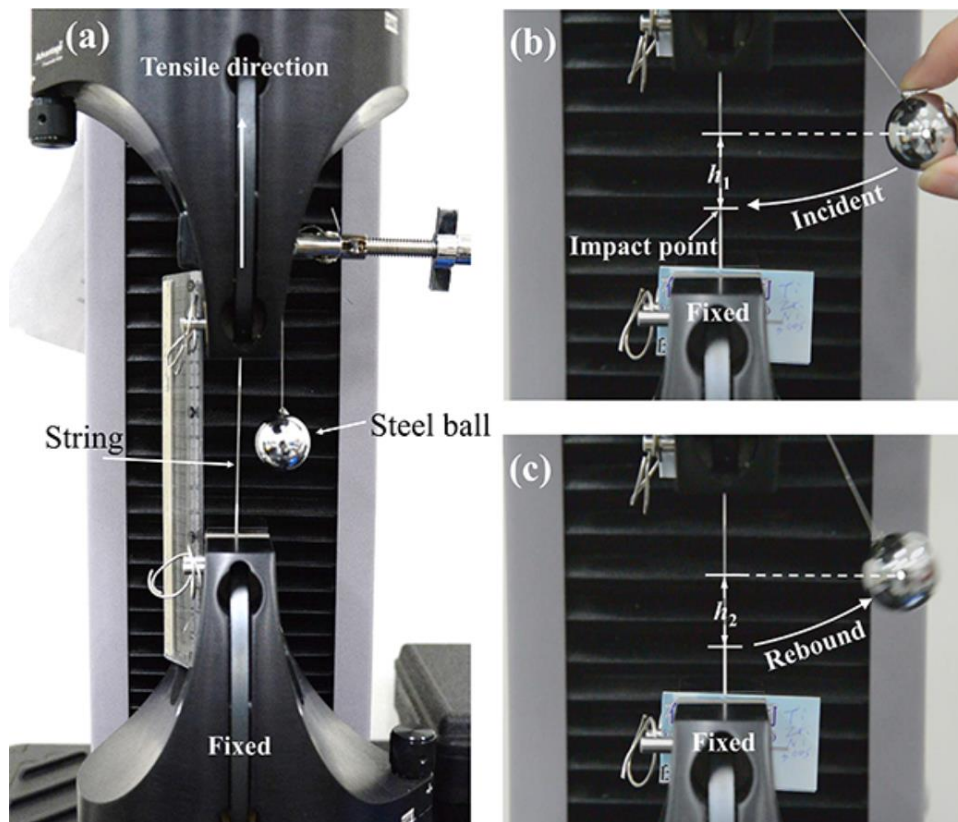


**Figure 2** (a) Setup of the modified ball-drop test, (b) the initial height,  $h_1$ , of the steel ball prior to release, and (c) the captured image depicting the rebound height,  $h_2$ , of the steel ball.

In the present study, in order to simulate different strung tensions in the string of the badminton racquet, the coated badminton string was fixed on a mechanical testing system (MTS, Criterion 42.503 model, USA) with constant tensile loading forces of 18, 20, 22, 24, and 26 pounds. The setup of the modified ball-drop test is depicted in Figure 2(a). The coated badminton string was loaded in tension. A steel ball was suspended using a string on the side of the coated string. The coated string under tensile loading and the string used for suspending the steel ball were carefully aligned to be coplanar. While conducting the test, the steel ball was raised to a height of  $h_1$  with respect to a reference point at which the steel ball would impact the coated string upon release [Figure 2(b)]. After impacting the coated string, the steel ball would rebound to a height of  $h_2$  [Figure 2(c)]. The whole process was recorded using a video camera in order to record the

height  $h_2$  reached upon rebound. The tensile strength of the coated badminton string was also measured using the same mechanical testing system and a loading rate of 1 mm/s.

### 3. Results and Discussion

#### 3.1 Composition and Structure of TFMG Coatings

Using EPMA, the compositions of Zr-based and Ti-based TFMGs were determined to be  $Zr_{58 \pm 0.2}Cu_{22 \pm 0.2}Al_{8 \pm 0.1}Ni_{10 \pm 0.1}$  and  $Ti_{49 \pm 0.5}Zr_{23 \pm 0.2}Ni_{28 \pm 0.5}$ , respectively. The X-ray diffraction patterns of the Zr-based and Ti-based TFMGs scanned in the range of  $20^\circ$ – $80^\circ$  are shown in Figure 3. Both the spectra presented a broad hump at  $\sim 40^\circ$  with no obvious diffraction peaks, which verified the amorphous nature of the films. The SEM micrographs of the cross-sections of the Zr-based and Ti-based TFMGs deposited on Si wafers for 120 min are shown in Figure 4(a) and 4(b), respectively. The thicknesses of the Zr-based and Ti-based TFMGs were 600 nm and 560 nm, respectively, and both the films were dense with no observable porosities. The corresponding SEM micrographs of the cross-sections of the Zr-based and Ti-based TFMGs deposited on strings for 120 min are shown in Figure 4(c) and Figure 4(d), respectively. The multifilament structure of the core of the string could be observed. The thicknesses of the Zr-based and Ti-based TFMGs were 340 nm and 292 nm, respectively. In consideration of the rotation of the string during the sputtering process, the string surface exposed to film deposition was approximately half of the deposition time. Therefore, for the same deposition time, the coating thickness on the string was approximately half of that on the flat Si wafer.

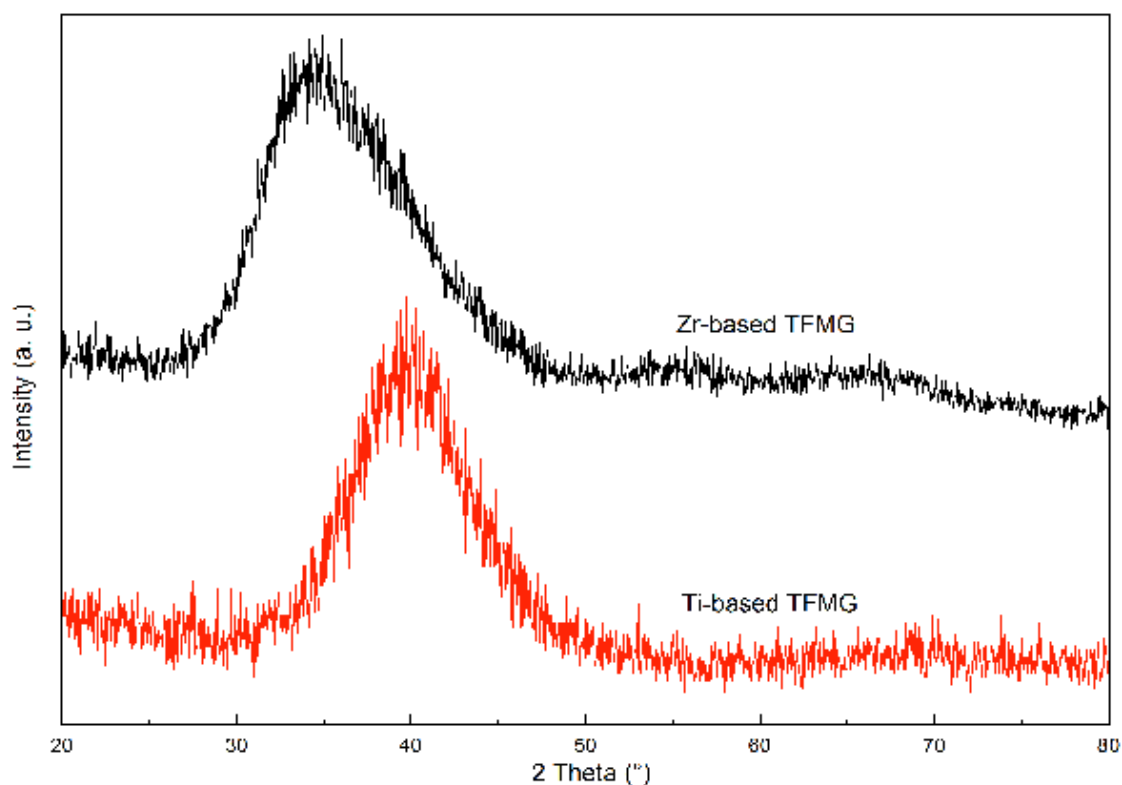


**Figure 3** X-ray diffraction patterns of Zr-based and Ti-based TFMGs.

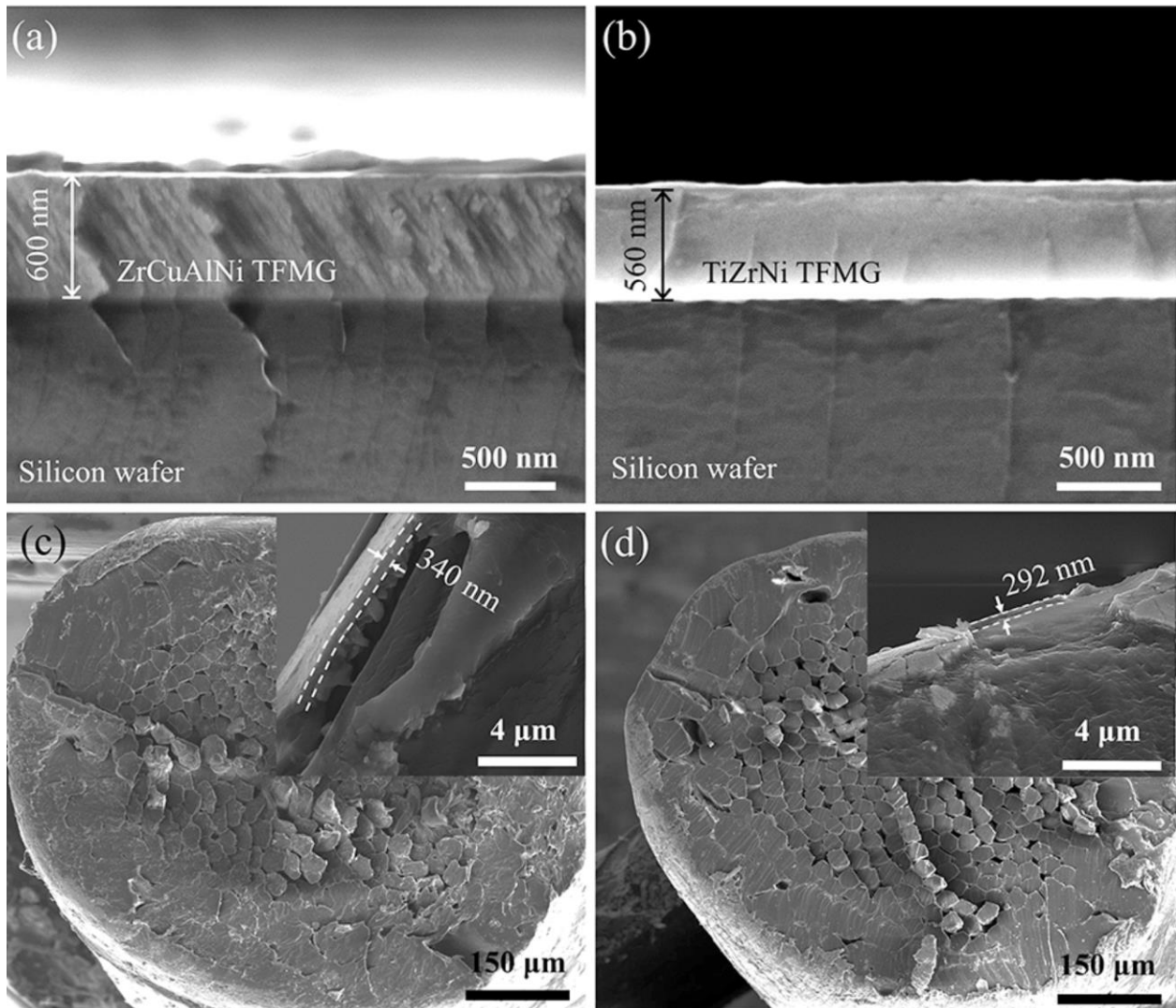


**Figure 4** SEM micrographs showing the cross-sections of (a) Zr-based and (b) Ti-based TFMGs deposited on Si wafer and of (c) Zr-based and (d) Ti-based TFMGs deposited on the rotated string for 120 min, with the inset displaying the coating thickness.

### 3.2 Morphology of TFMG Coating on a String

Surface morphologies of the strings coated with Zr-based and Ti-based TFMGs for different deposition time were observed under an optical microscope and are shown in Figure 5. In Figure 5(a), fiber braiding of the string without a TFMG coating could be observed. All the coated strings exhibited metallic luster. Although the surfaces of the coated strings were smooth for the coating time of 5 min and 30 min, cracks appeared on the string surfaces for the coating time of 60 min and 120 min, for both Zr-based and Ti-based TFMG coatings. This cracking could be attributed to the residual stresses developed upon film deposition and cooling down from the deposition temperature.

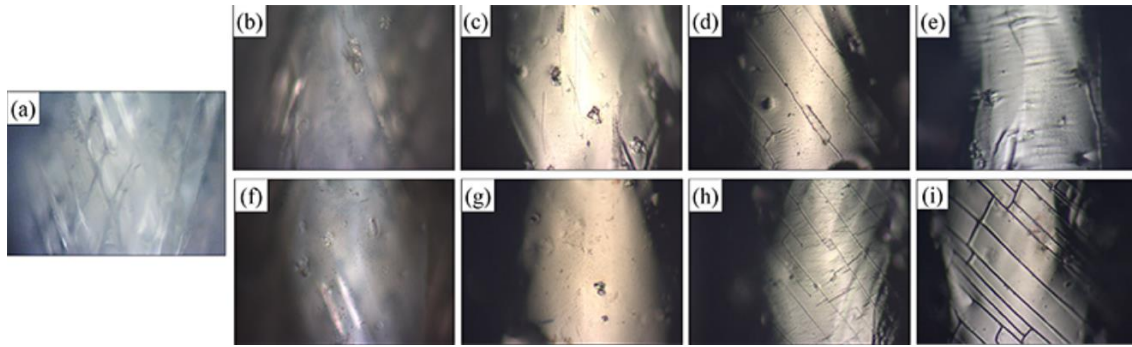


**Figure 5** The optical microscope images of the strings coated with Zr-based and Ti-based TFMGs for different deposition time: (a) Pristine BG65 string without a TFMG coating, (b)-(e) Strings coated with Zr-based TFMGs for 5 min, 30 min, 60 min, and 120 min, respectively, (f)-(i) Strings coated with Ti-based TFMGs for 5 min, 30 min, 60 min, and 120 min, respectively.

### 3.3 Modified Ball-Drop Test

In order to study the energy loss and determine the COR, a steel ball with a diameter of 2.2 cm and weight 45.35 g was released to impact the tightened string from the side (Figure 2), while the process was recorded using a video camera (D800, Nikon). The recorded video of this modified ball-drop test is available for viewing at Video S1.mp4 in the Supplementary Materials. In order to ensure a coplanar head-on impact between the steel ball and the coated string, the data for the first rebound were considered only when the steel ball could rebound from the string at least three times. In this case, the relative potential energies of the initial ball position prior to releasing and after the first rebound were  $mgh_1$  and  $mgh_2$ , respectively, where  $m$  denoted the mass of the ball and  $g$  is the gravitational acceleration. Therefore, the energy loss due to the rebound,  $\Delta E$ , is represented by the following equation:

$$\Delta E = mg(h_1 - h_2) \quad (1)$$

The COR is a measure of the restitution of a collision between the ball and the string. When the steel ball was released from its initial position to impact the string, the potential energy of the ball,  $mgh_1$ , was converted into kinetic energy,  $mv_1^2/2$ , where  $v_1$  denotes the incident velocity of the ball upon impacting the string. As a consequence of the energy loss of the steel ball at impact, the ball would rebound with a velocity  $v_2$ . The kinetic energy of the rebounded ball,  $mv_2^2/2$ , would convert into potential energy,  $mgh_2$ , when the ball would reach the maximum rebound height  $h_2$ . The coefficient of restitution (COR) is defined as the ratio between the rebound velocity and the incident velocity, and is expressed as follows [26-31]:

$$\text{COR} = \frac{v_2}{v_1} = \sqrt{\frac{h_2}{h_1}} \quad (2)$$

As  $h_1$  and  $h_2$  were recorded during the modified ball-drop test, these could be used to calculate the energy loss  $\Delta E$  and COR from the equations (1) and (2), respectively. In the present study, the success rate of the modified ball-drop tests was approximately 20%, and the results presented here were based on at least four successful tests for each case. The normalized energy loss,

$\Delta E/mgh_1$ , as a function of tensile loading on the string, for the strings coated for different coating time with Zr-based TFMGs and Ti-based TFMGs is presented in Figure 6(a) and Figure 6(b), respectively. Figure 6 demonstrates that energy loss decreased with increasing tensile loading on the string. However, for both Zr-based and Ti-based TFMG coatings, the energy loss initially decreased with the coating time and then increased when the coating time reached 60 min; the deposition time of 30 min presented the lowest energy loss observed in the present study. The above-stated results could be interpreted using the micrographs shown in Figure 5. While the TFMG coating could reduce the energy loss at impact, cracking of TFMG would degrade its functionality. The COR corresponding to the normalized energy loss shown in Figure 6 is presented in Figure 7. Lower energy loss would result in a higher COR. The best COR, presented in Figure 7(b), was 0.985, obtained for the Ti-based coating for deposition time of 30 min and the string tension of 26 lb. It is noteworthy that the surface morphologies of the coated strings shown in Figure 5 did not reveal observable changes after the modified ball-drop tests for the coating time of 5 min and 30 min. However, a few more cracks could be observed after the tests for the coating time of 60 min and beyond. In addition, while the normalized energy loss demonstrated a slightly increasing trend and the COR demonstrated a slightly decreasing trend with the increasing number of tests for the films with the coating time of 60 min and beyond, no trend could be concluded for the films with the coating time of 0 min, 5 min, and 30 min.

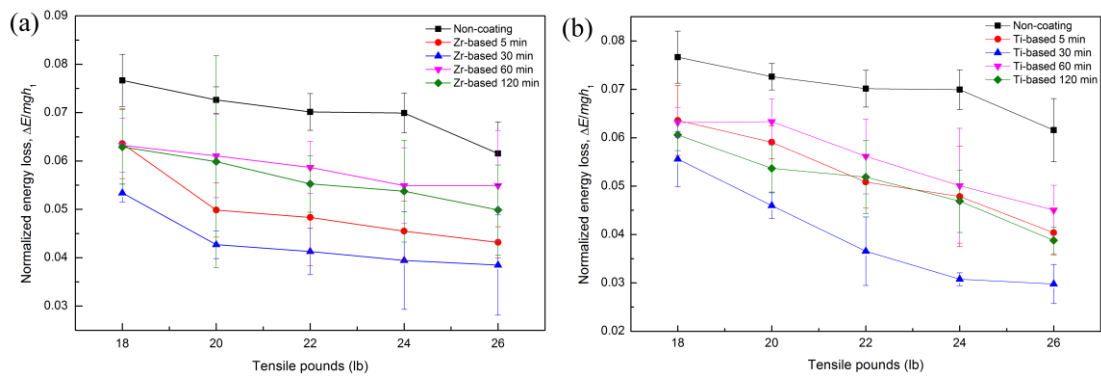


**Figure 6** The normalized energy loss,  $\Delta E/mgh_1$ , as a function of tensile loading for (a) Zr-based and (b) Ti-based TFMG coated strings with different coating time.

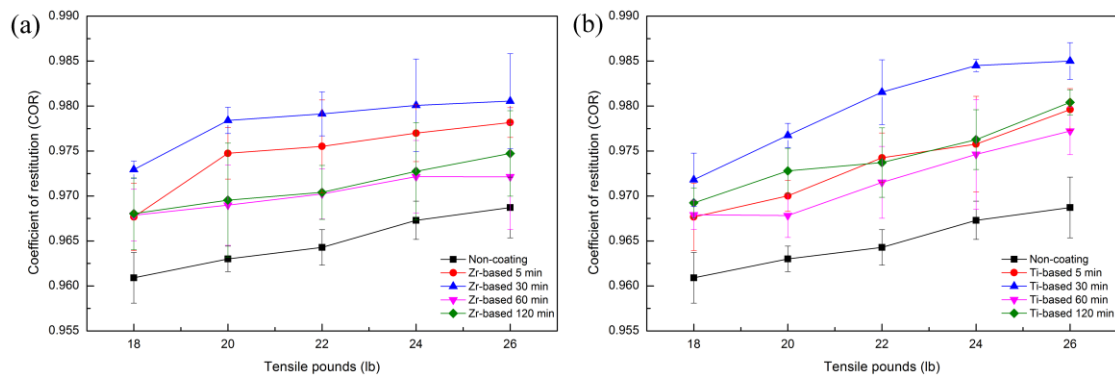


**Figure 7** The COR as a function of tensile loading for (a) Zr-based and (b) Ti-based TFMG coated strings with different coating time.

### 3.4 Tensile Strength of the Coated String

Stress analyses of tensile loading on a coated fiber have been performed previously [32]. Failure of the coated fiber could result from the segmentation of the coating, debonding at the fiber/coating interface, or fracture of the fiber, depending on the material properties and the coating thickness. The tensile load-displacement curves for the Zr-based and Ti-based TFMG coated strings are presented in Figure 8(a) and Figure 8(b), respectively, for different coating time. The fracture strengths of the strings were in the range of 45–57 lb. In consideration of statistical errors, no trend could be observed for the effects of coating thickness on the tensile strength of the string. Theoretically, the strength of the string should increase with a high-strength coating. However, compared to the string diameter of 0.7 mm, the coating thickness of less than 350 nm is too thin to exert any noticeable effects on the tensile strength of the string according to the rule-of-mixtures.

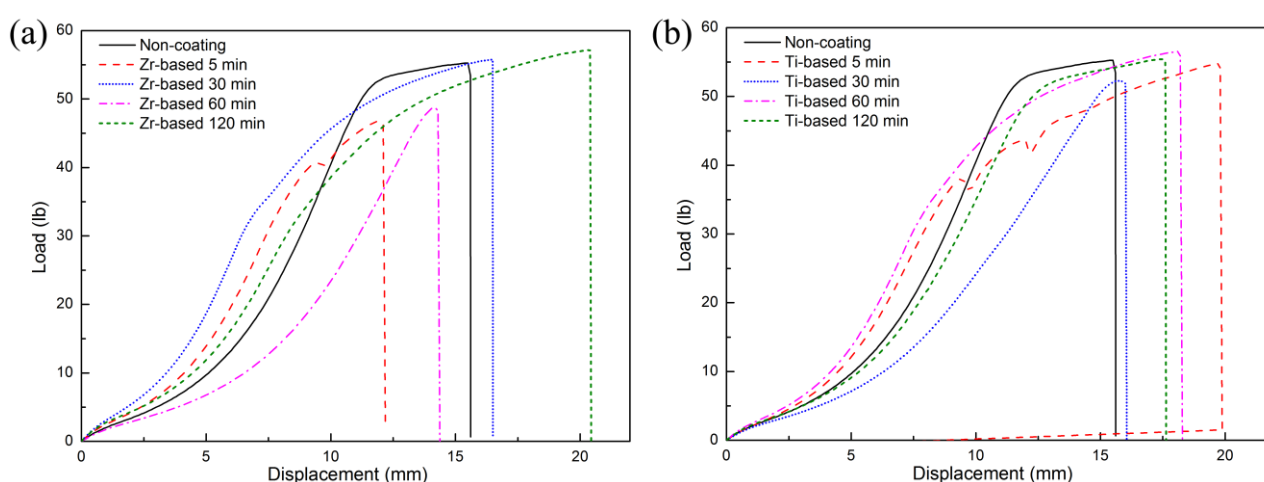


**Figure 8** Tensile load-displacement curves for (a) Zr-based and (b) Ti-based TFMG coated strings with different coating time.

#### 4. Conclusions

In the present work, Zr-based and Ti-based TFMGs were successfully coated on BG65 badminton strings using sputtering. The compositions of the as-deposited Zr-based TFMG and Ti-based TFMG were  $Zr_{58}Cu_{22}Al_8Ni_{10}$  and  $Ti_{49}Zr_{23}Ni_{28}$ , respectively. However, cracking of the deposited films occurred at the deposition time of 60 min and beyond. The amorphous structure of the film was verified using X-ray diffraction. In order to simulate the strung tension of the string in the racquet, the coated string was subjected to different pounds of tensile loading and was subsequently impacted using a steel ball in a modified ball-drop test (Figure 2) to study both energy loss and the coefficient of restitution (COR). It was observed that while the TFMG coating could reduce the energy loss and increase the COR, it exerted negligible effects on the tensile strength of the badminton string. In addition, there existed an optimum TFMG coating thickness, beyond which cracking of the coating would occur and degrade the beneficial effects of the coating. The present work demonstrated the potential of using TFMG coatings to reduce energy loss and increase the COR of the strings in sports equipment at impact. While the present study evaluated the impact between a ball and a coated string for the application of strings in racquet sports, it would be interesting to study the application of these coated strings in musical

instruments; in the latter case, strings subjected to frictional loading should be considered, and an experimental setup based on fretting fatigue testing of strings [33] could be designed.

### **Author Contributions**

Yi-Chia Liao: Investigation, Methodology, Writing-original draft. Chun-Hway Hsueh: Supervision, Writing-review & editing, Funding acquisition. Wen-Shin Lee: Conceptualization, Supervision, Writing-review & editing, Funding acquisition.

### **Funding**

This work was jointly supported by National Taiwan University under Project no. T105E2030007 and the Ministry of Science and Technology, Taiwan under Contract no. MOST 106-2221-E-002-072-MY2.

### **Competing Interests**

The authors have declared that no competing interests exist.

### **Additional Materials**

The following additional material is uploaded at the page of this paper.

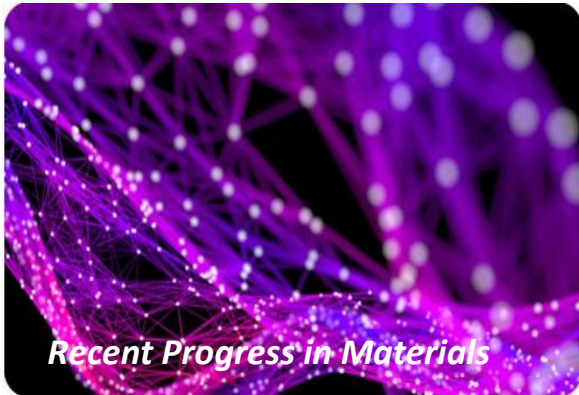
1. Video S1.mp4: Modified Ball-Drop Test.

### **References**

1. Badminton. Wikipedia, the free encyclopedia; 2020 [cited date 2020 May 16]. Available from: <https://en.wikipedia.org/wiki/Badminton>
2. Badminton String. K.L, Malaysia: Badminton Information; 2012 [cited date 2020 May 16]. Available from: [http://www.badminton-information.com/badminton\\_string.html](http://www.badminton-information.com/badminton_string.html)
3. BG65 Titanium. Tokyo: YONEX; 2020 [cited date 2020 May 16]. Available from: <http://www.yonex.com/products/badminton/string/strings/bg65ti/>
4. Klement W, Willens RH, Duwez P. Non-crystalline structure in solidified gold-silicon alloys. *Nature*. 1960; 187: 869-870.
5. Johnson WL. Bulk glass-forming metallic alloys: Science and technology. *MRS Bull*. 1999; 24: 42-56
6. Inoue A. Stabilization of metallic supercooled liquid and bulk amorphous alloys. *Acta Mater*. 2000; 48: 279-306.
7. Miller M, Liaw PK. *Bulk Metallic Glasses-An Overview*. New York: Springer Science & Business Media; 2008.
8. Huang JC, Chu JP, Jang JSC. Recent progress in metallic glasses in Taiwan. *Intermetallics*. 2009; 17: 973-987.
9. Suryanarayana C, Inoue A. *Bulk Metallic Glasses*. 2nd ed. Boca: Taylor & Francis Group; 2011.
10. Telford M. The case for bulk metallic glass. *Mater Today*. 2004; 7: 36-43.
11. Choi YC, Hong SI. Mechanical properties and microstructure of commercial amorphous golf club heads made of Zr-Ti-Cu-Ni-Be bulk metallic glass. *Mater Sci Eng A*. 2007; 449-451: 126-129.

12. Chang SY, Lee YS, Hsiao HL, Chang TK. Mechanical properties and deformation behavior of amorphous nickel-phosphorous films measured by nanoindentation test. *Metall Mater Trans A*. 2006; 37: 2939-2945.
13. Chen CJ, Huang JC, Chou H, Lai YH, Chang LW, Du XH, et al. On the amorphous and nanocrystalline Zr-Cu and Zr-Ti co-sputtered thin films. *J Alloy Compd*. 2009; 483: 337-340.
14. Chen CS, Yiu P, Li CL, Chu JP, Shek CH, Hsueh CH. Effects of annealing on mechanical behavior of Zr-Ti-Ni thin film metallic glasses. *Mater Sci Eng A*. 2014; 608: 258-264.
15. Hata S, Sakurai J, Shimokohbe A. Thin film metallic glasses as new MEMS materials. 18th IEEE International Conference on MEMS; 2005 July 05; Miami Beach, FL, USA. IEEE. p.479-482.
16. Chu JP, Jang JSC, Huang JC, Chou H, Yang Y, Ye JC, et al. Thin film metallic glasses: Unique properties and potential applications. *Thin Solid Films*. 2012; 520: 5097-5122.
17. Chiang CL, Chu JP, Liu FX, Liaw PK, Buchanan RA. A 200 nm thick glass-forming metallic film for fatigue-property enhancements. *Appl Phys Lett*. 2006; 88: 131902.
18. Diyatmika W, Chu JP, Yen YW, Chang WZ, Hsueh CH. Thin film metallic glass as an underlayer for tin whisker mitigation: A room temperature evaluation. *Thin Solid Films*. 2014; 561: 93-97.
19. Wang CW, Yiu P, Chu JP, Shek CH, Hsueh CH. Zr-Ti-Ni thin film metallic glass as a diffusion barrier between copper and silicon. *J MaterSci*. 2015; 50: 2085-2092.
20. Chu JP, Yu CC, Tanatsugu Y, Yasuzawa M, Shen YL. Non-stick syringe needles: Beneficial effects of thin film metallic glass coating. *Sci Rep*. 2016; 6: 31847.
21. Yu CC, Wu HJ, Deng PY, Agne MT, Snyder GJ, Chu JP. Thin-film metallic glass: An effective diffusion barrier for Se-doped AgSbTe<sub>2</sub> thermoelectric modules. *Sci Rep*. 2017; 7: 45177.
22. Li S, Horikawa S, Park MK, Chai Y, Vodyanoy VI, Chin BA. Amorphous metallic glass biosensors. *Intermetallics*. 2012; 30: 80-85.
23. Chao BK, Xu Y, Ho HC, Yiu P, Lai YC, Shek CH, et al. Gold-rich ligament nanostructure by dealloying Au-based metallic glass ribbon for surface-enhanced Raman scattering. *Sci Rep*. 2017; 7: 7485.
24. Wang C, Nien LW, Ho HC, Lai YC, Hsueh CH. Surface plasmon excited on imprintable thin film metallic glasses for surface-enhanced Raman scattering applications. *ACS Appl Nano Mater*. 2018; 1: 908-914.
25. Yiu P, Diyatmika W, Bonninghoff N, Lu YC, Lai BZ, Chu JP. Thin film metallic glasses: Properties, applications and future. *J Appl Phys*. 2020; 127: 030901.
26. Haron A, Ismail KA. Coefficient of restitution of sports balls: A normal drop test. *IOP Conf Ser Mater Sci Eng*. 2012; 36: 012038.
27. Persson J. Measure the coefficient of restitution for sports balls. *Phys Educ*. 2012; 47: 662-663.
28. Wadhwa A. Measuring the coefficient of restitution using a digital oscilloscope. *Phys Educ*. 2009; 44: 517-521.
29. Cross R. The bounce of a ball. *Am J Phys*. 1999; 67: 222-227.
30. Aryaei A, Hashemnia K and Jafarpur K. Experimental and numerical study of ball size effect on restitution coefficient in low velocity impacts. *Inter J Impact Eng*. 2010; 37: 1037-1044.
31. Nasruddin FA, Harun MN, Syahrom A, Abdul Kadir MR, Omar AH, Öchsner A. Finite element analysis on badminton racket design parameters. New York: Springer; 2016. p.15-26.
32. Hsueh CH. Analytical evaluation of interfacial shear strength for fiber-reinforced ceramic composites. *J Am Ceram Soc*. 1988; 71: 490-493.

33. Phong LM. Non-destructive testing of tennis strings. *Vietnam J Mech.* 2009; 30: 319-327.



Enjoy *Recent Progress in Materials* by:

1. [Submitting a manuscript](#)
2. [Joining in volunteer reviewer bank](#)
3. [Joining Editorial Board](#)
4. [Guest editing a special issue](#)

For more details, please visit:

<http://www.lidsen.com/journals/rpm>